

Design and Fabrication of a Novel Bimorph Micro-Opto-Mechanical Sensor

Si-Hyung Lim, Jongeun Choi, Roberto Horowitz, *Member, IEEE*, and Arunava Majumdar, *Fellow, ASME*

Abstract—We have designed a so-called Flip-Over Bi-material (FOB) beam to increase the sensitivity of micro-mechanical structures for sensing temperature and surface stress changes. The FOB beam has a configuration such that a material layer coats the top and bottom of the second material at different regions along the beam length. By multiple interconnections of FOB beams, the deflection or sensitivity can be amplified, and the out-of-plane motion of a sensing structure can be achieved. The FOB beam has 53 % higher thermo-mechanical sensitivity than a conventional one. Using the FOB beam design, we have developed a micro-opto-mechanical sensor having a symmetric structure such that beam deflection is converted into a linear displacement of a reflecting surface, which is used for optical interferometry. The designed sensor has been fabricated by surface micromachining techniques using a transparent quartz substrate for optical measurement. Within a sensor area of $100 \mu\text{m} \times 100 \mu\text{m}$, the thermo-mechanical sensitivity $S_T = 180 \text{ nm/K}$ was experimentally obtained.

Index Terms—Flip-Over Bi-material (FOB) beam, temperature sensing, surface stress sensing, out-of-plane motion, thermo-mechanical sensitivity, interferometry, surface micromachining, quartz substrate.

I. INTRODUCTION

A micro-cantilever based sensor can detect extremely small external stimuli that include temperature and surface stress changes. It has found several applications in thermal and infrared [1], [2], chemical [2], [3], [4], and biological sensing [2], [5], [6]. In all these cases, the cantilever produces either a static deflection or its resonance frequency changes. Deflection sensing methods can be divided into two categories: electrical [4] and optical [1], [6], [7]. Although the electrical method, including capacitance and piezo-resistive sensing, is promising due to its compatibility with electric signal processing, it is limited due to lack of thermal isolation and Johnson noise [1]. Furthermore, for piezo-resistive sensing, there are technological limits in fabricating a thin, highly sensitive cantilever [8]. The most common readout techniques for cantilever motion are optical including optical lever [6], [7], [9] and interferometric methods [1], [10]. These optical methods can detect cantilever motion with sub-Angstrom resolution limited only by thermal vibrational noise [7], [10].

For both temperature and surface stress change, the amount of cantilever deflection, h , is proportional to the square of the cantilever length, L , or $h \sim L^2$. Also, the resolution is limited by the thermal vibrational noise, $h_n = \sqrt{2k_B T B / K \pi f_o Q}$, where k_B is the Boltzmann constant, T is the absolute temperature, B is the measurement bandwidth, f_o is the resonance frequency, K is the cantilever stiffness, and Q is the quality factor of the resonance, which is related to damping. Cantilever sensors become more sensitive with increased cantilever length, L . However,

This work was supported by Department of Energy Environmental Management Science Program (DOE-EMSP).

Authors are with the Department of Mechanical Engineering, University of California, Berkeley, CA94720 USA (e-mail:majumdar@me.berkeley.edu).

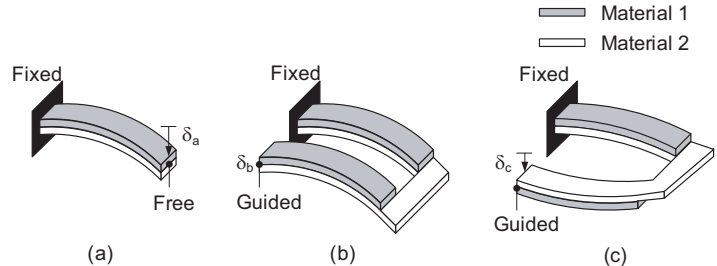


Fig. 1. Deformation shape of a single bi-material cantilever and double connected bi-material beams for temperature or surface stress change. δ_i ($i=a,b,c$) is the vertical deflection amount of each case.

lower spring constant, K , and resonance frequency, f_o , resulting from an increased length, also increase the thermal vibrational noise, h_n . Since a serpentine structure is stiffer than a straight structure for the same total structural length, a promising approach to increase cantilever sensitivity without a significant increase of the thermal vibrational noise is to connect multiple bi-material beams in a serpentine manner. Fig. 1 shows the deformation of a single bi-material cantilever (a) and double connected bi-material beams under fixed-guided boundary conditions (b), (c), where the deformation can be generated by either temperature or surface stress change. Fig. 1(b) shows serially connected bi-material beams, each of which has material 1 on top of material 2. The end point under guided boundary condition has almost zero deflection, or $\delta_b \sim 0$. Therefore, nothing is gained from using multiple interconnections. Fig. 1(c) also shows serially connected bi-material beams, one of which has material 1 on top of material 2, and the other has material 1 on bottom of material 2. The end point has a smaller vertical deflection than the end point 'a' of Fig. 1(a), or $\delta_c \sim 0.2\delta_a$. Therefore, by using simple bi-material beam interconnection methods, it is not possible to achieve a higher end point deflection as compared to a single bi-material cantilever.

In this paper, we propose a novel flip-over bi-material (FOB) beam design to achieve a higher sensitivity in a finite sensor region. Also, we propose a bimorph micro-opto-mechanical sensor using the FOB beam design. This sensor is fabricated by surface micromachining using a transparent quartz substrate for optical measurement.

II. DESIGN

A. FOB Beam Design

To increase the mechanical deflection of a bi-material sensing structure in a finite sensor region, we propose a new bi-material beam design, which can be serially interconnected with other beams at the same design to increase out-of-plane displacement of the structure. Fig. 2 shows the proposed FOB beam design under a

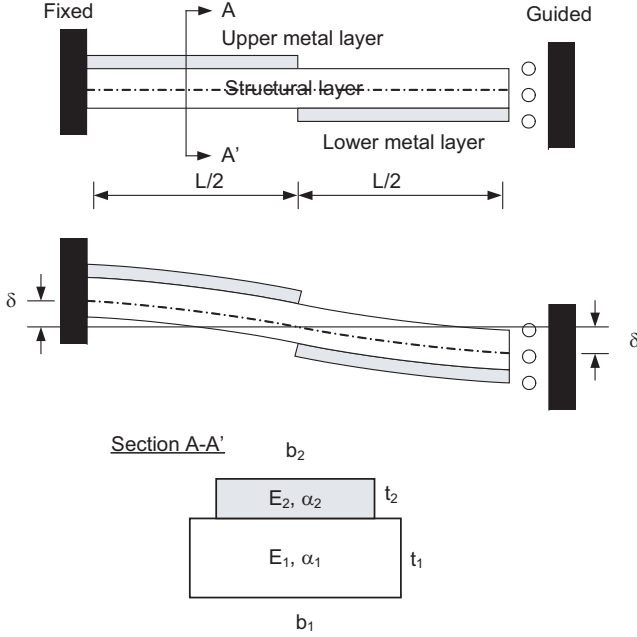


Fig. 2. Flip-over bi-material (FOB) beam design

fixed-guided boundary condition. For half of the structure, a metal layer is located above the structural layer, while in the other half, the metal layer is located below it. It should be noted that the FOB beam structure automatically satisfies the fixed-guided boundary condition due to symmetry. Since the end point of the FOB beam is flat, or zero slope, by the fixed-guided boundary condition, the end point deflection is purely vertical. This deflection can be greatly enhanced by multiple connections of the same FOB beams. The total deflection of multiply connected FOB beam structures can be approximated as the addition of each FOB beam deflection.

Since the radius of curvature of each half bi-material beam structure is the same, the deflection of each beam is the same. Therefore, the total deflection Δh_t due to a temperature change ΔT can be calculated as two times the deflection of a bi-material beam having length $L/2$. The proposed FOB beam having length L in the fixed-guided boundary condition has the following thermal deflection Δh_t .

$$\begin{aligned} \Delta h_t &\approx \frac{1}{2} \kappa_t (L/2)^2 \times 2 \\ &= \frac{1}{4} \kappa_t L^2, \end{aligned} \quad (1)$$

where, κ_t is the thermally induced curvature of the bi-material cantilever beam having the cross-section given in Fig. 2 and it can be calculated as follows [11], [12].

$$\begin{aligned} \kappa_t &= \\ &\frac{6b_1b_2E_1E_2t_1t_2(t_1+t_2)(\alpha_2-\alpha_1)}{(b_1E_1t_1^2)^2 + (b_2E_2t_2^2)^2 + 2b_1b_2E_1E_2t_1t_2(2t_1^2 + 3t_1t_2 + 2t_2^2)} \\ &\times \Delta T, \end{aligned} \quad (2)$$

where, b_i , E_i , t_i , and α_i ($i = 1, 2$) are respectively width, Young's modulus, thickness, and thermal expansion coefficient of each layer. In some applications like chemical or biological sensing, the purpose of the metal layer is only to permit molecular adsorption

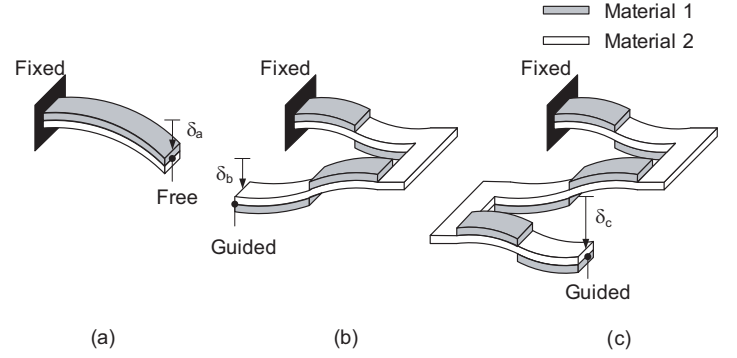


Fig. 3. Deformation shape of a single bi-material cantilever and multiply connected FOB beams for temperature or surface stress change. δ_i ($i=a,b,c$) is the vertical deflection amount of each case.

or binding [2], [4], [5], [6]. Its thickness, t_2 is generally very thin ($\sim 30\text{nm}$) as compared to the structural layer thickness, t_1 ($t_2 \ll t_1$). Therefore, the effect of the metal layer on the deflection can be neglected. The deflection Δh_s by surface stress change $\Delta\sigma$, which is induced by molecular adsorption or binding, can be expressed as

$$\begin{aligned} \Delta h_s &\approx \frac{1}{2} \kappa_s (L/2)^2 \times 2 \\ &= \frac{1}{4} \kappa_s L^2, \end{aligned} \quad (3)$$

where, κ_s is the curvature induced by surface stress, and it can be calculated as follows [13].

$$\kappa_s = \frac{6(1-\nu_1)}{E_1t_1^2} \Delta\sigma, \quad (4)$$

where, ν_1 is the Poisson's ratio of the structural layer given in Fig. 2. From (1) and (3), we can easily check that the deflection of the FOB beam structures can be higher than that of a cantilever beam if more than two FOB beams are used. Fig. 3 shows the vertical deflection of multiply connected FOB beams. Fig. 3(b) shows double connected FOB beams, and its deflection δ_b is equal to δ_a . Also, Fig. 3(c) shows triple connected FOB beams, and its deflection δ_c is 1.5 times δ_a , or $\delta_c \sim 1.5\delta_a$. The performance of the proposed FOB beam design can be compared with that of a conventional bi-material beam design having the same fixed-guided boundary condition. The conventional bi-material beam has only one metal layer on top of the structural layer. For the fixed-guided boundary condition, when the metal layer coats almost half of the structural layer length, the end point deflection is maximized. As an example, Fig. 4 shows the end point deflection of a conventional bi-material beam, which has a gold metal layer on top of the silicon nitride structural layer, for various gold layer coverage length L_{Au} . Table I shows the material properties of gold and silicon nitride film [12], [14], [15], [16]. Finite element simulation shows the maximum deflection $\Delta h = 3.48 \mu\text{m}$ at $L_{Au} = 60 \mu\text{m}$ for the overall temperature change $\Delta T = 100 \text{K}$. On the other hand, finite element simulation result for the proposed FOB beam design shows that the end point deflection is $5.31 \mu\text{m}$ for the same material properties, structural beam length $L = 100 \mu\text{m}$, and temperature change $\Delta T = 100 \text{K}$. Therefore, if we define the thermo-mechanical sensitivity S_T as mechanical deflection for a temperature change, the thermo-mechanical sensitivity

TABLE I
SIMULATION PARAMETERS

Contents	Au	SiNx	Unit
Thickness	0.2	0.5	μm
E	70	100	GPa
α	14.2	0.8	$\times 10^{-6}\text{K}^{-1}$
ν	0.35	0.27	

of the proposed FOB beam is $S_T = 53.1 \text{ nm/K}$ and that of the conventional beam is $S_T = 34.8 \text{ nm/K}$. This results in a performance increase of about 53 % by the FOB beam design. The analytical result from the model given by (1) is $S_T = 47.5 \text{ nm/K}$, which agrees within 11 % of the finite element simulation result.

Here, we emphasize the advantages of the proposed FOB

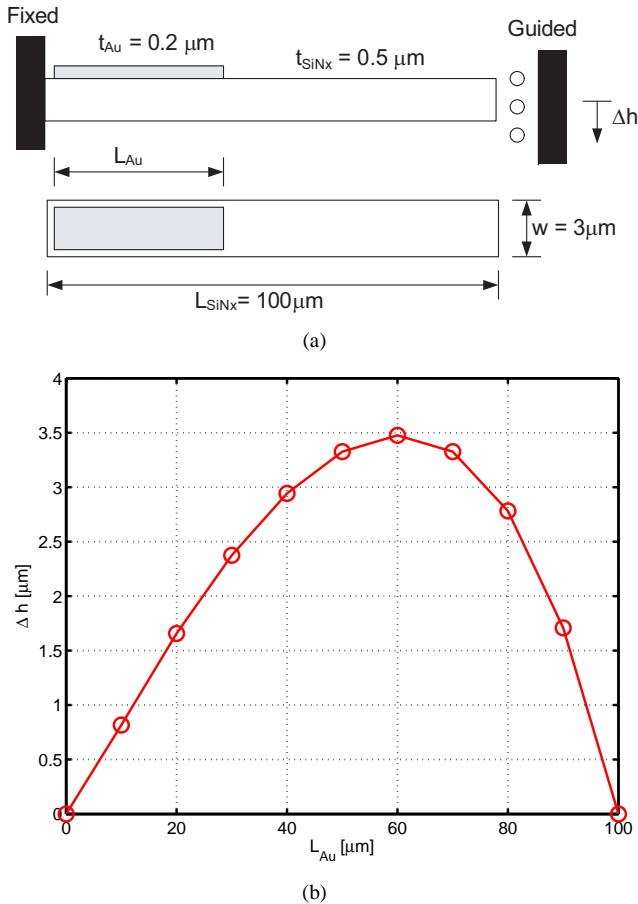


Fig. 4. The end point deflection of a conventional bi-material beam having a fixed-guided boundary condition (temperature change $\Delta T = 100 \text{ K}$): (a) conventional bi-material beam having fixed-guided boundary condition (b) finite element simulation for end point deflection vs. various gold coating length L_{Au}

beam design. First, the FOB beam itself can greatly enhance mechanical sensitivity when compared with a conventional bi-material beam having the same fixed-guided boundary condition. Second, total deflection is approximately proportional to the number of connections of FOB beams. Third, the displacement is purely translational without any rotation, which is ideal for optical interferometry.

B. Micro-Opto-Mechanical Sensor

Fig. 5 shows a micro-opto-mechanical sensor that is based on the FOB beam design. It consists of multiple interconnections of FOB beams, a moving mirror connected to two sets of multiple FOB beams, a fixed mirror on top of a quartz substrate, and two anchors. This overall sensor design includes several key features. The first is that optical sensing takes place through a transparent substrate. This has potential advantages in remote thermal radiation sensing. For infrared radiation sensing, we can increase the infrared energy absorption rate by almost 100 % by the simple addition of an IR absorption pad on top of the moving mirror. The second feature is the high mechanical sensitivity and pure vertical motion generated by FOB beams. Furthermore, it can be easily expanded to an array approach: multiple sensors and simultaneous optical measurements. Fig. 6 shows a finite element simulation result of the motion of the sensor due to temperature change using gold and silicon nitride as a metal layer and a structural layer, respectively. The entire sensor size is $100 \mu\text{m} \times 100 \mu\text{m}$, and the width of an FOB beam is $3 \mu\text{m}$. Also, the moving mirror size is $52 \mu\text{m} \times 52 \mu\text{m}$. Table I shows the gold and silicon nitride parameters used in this overall sensor simulation. In this structural simulation, we increased the overall sensor temperature by 1 K. The moving mirror exhibits pure vertical motion, as expected, and its vertical displacement is about 133 nm. Therefore, the mirror height change to the sensor temperature change is determined to be $S_T = 133 \text{ nm/K}$. The analytical calculation result using (1) gives us $S_T = 114 \text{ nm/K}$, which agrees within 14 % of the finite element simulation result. Additionally, modal analysis showed the first resonance frequency to be at 6.1 kHz. Also, a spring constant of 0.1 N/m was obtained from the static structural finite element analysis. Furthermore, the thermal vibrational noise, h_n , is 0.036 nm for a quality factor $Q \sim 10$ in an atmospheric environment and a measurement bandwidth $B = 3 \text{ kHz}$. This corresponds to noise equivalent temperature resolution of $\Delta T_n = h_n/S_T = 271 \mu\text{K}$.

The optical interferometric signal from the moving and the fixed mirrors can be expressed as [1], [10]

$$I \sim \cos^2 \frac{\phi}{2}, \quad (5)$$

where, ϕ is

$$\phi = \frac{4\pi h}{\lambda}, \quad (6)$$

where, h is the height difference between the fixed mirror and the moving mirror, and λ is the wave length of the light source used. Noting that the height difference h can be expressed as $S_T \cdot \Delta T$ and thermo-mechanical sensitivity S_T is 133 nm/K, the proposed sensor will have a maximum to minimum light intensity change for a sensor temperature change $\Delta T = \lambda/4S_T = 1.2 \text{ K}$ for the light wave length $\lambda = 632.8 \text{ nm}$ (He-Ne laser). Hence, to make noise-equivalent temperature measurement, we would require a $\log(1.2/2.71 \times 10^{-4})/\log(2) \approx 12$ bit CCD camera. Table II summarizes all the finite element simulation and calculated results explained above.

III. FABRICATION

We have fabricated the micro-opto-mechanical sensor using surface micro-machining techniques. The general fabrication approach is as follows. First, a quartz substrate is used as an

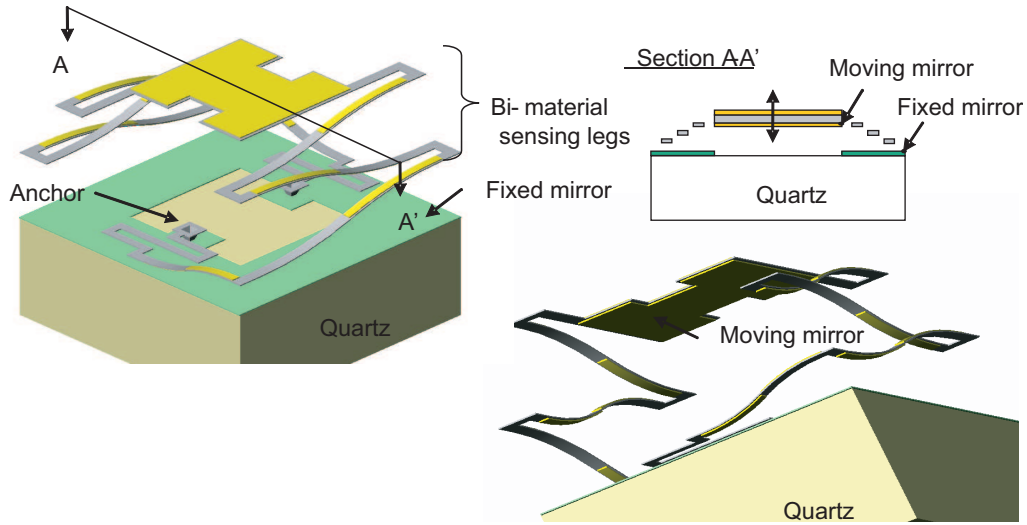


Fig. 5. Proposed micro-opto-mechanical sensor using FOB beam design

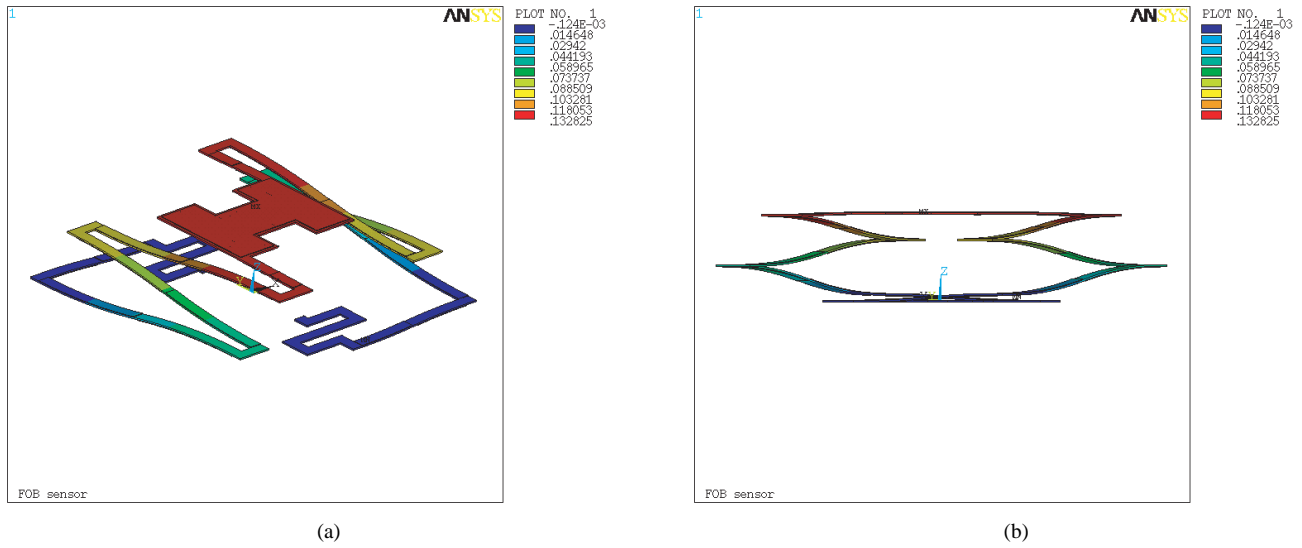


Fig. 6. Proposed micro-opto-mechanical sensor finite element simulation results using ANSYS (the deformation shape is exaggerated in the vertical direction): (a) perspective view (b) side view

TABLE II

SUMMARY OF FINITE ELEMENT SIMULATION AND CALCULATED RESULTS

Contents	FEM	Comment
S_T	133 nm/K	Thermo-mechanical sensitivity
ω_n	6.1 kHz	Natural frequency
k	0.1 N/m	Spring constant
h_n	0.036 nm	Thermal vibrational noise
ΔT_n	271 μ K	Noise-equivalent temperature resolution (h_n/S_T)
ΔT	1.2 K	Temperature dynamic range

optically transparent layer. Second, a poly-Ge film is used as a sacrificial layer, since it is compatible with low temperature process and is highly selective to gold, silicon nitride, and quartz in XeF_2 etching. Finally, ECR (Electron Cyclotron Resonance) PECVD is used for low temperature silicon nitride deposition. Fig. 7 shows the detailed fabrication process. 0.2 μm thick aluminum layer was evaporated, then patterned using an aluminum wet etchant (Fig. 7(a)). A poly-Ge furnace deposited 2 μm thick poly-Ge layers on both sides of the quartz wafer. Then, the upper

poly-Ge layer was patterned using a reactive ion etching method (Fig. 7(b)). For a lower metal layer, 0.2 μm thick gold and 10 nm thick chromium were evaporated sequentially, and then patterned by a lift-off technique (Fig. 7(c)). Using the ECR PECVD, 0.5 μm thick silicon nitride was deposited as a structural layer. Then, the silicon nitride layer was etched by a reactive ion etching method (Fig. 7(d)). For an upper metal layer, 10 nm thick chromium and 0.2 μm thick gold were evaporated sequentially, and then patterned by a lift-off technique (Fig. 7(e)). In the fabrication process (c) and (e), the thin chromium layers were used to promote adhesion between gold and silicon nitride. Finally, the sacrificial layer, poly-Ge, was etched by a dry etching method using XeF_2 gas (Fig. 7(f)).

During the whole fabrication process, low temperatures were used. Therefore, we could minimize the thermal residual stress caused by high temperature processing. Fig. 8 shows the SEM picture of the fabricated chip and Fig. 9 shows the chip back side image through the transparent quartz substrate. As shown in Fig. 8, after release, the moving mirror moved up to about 13

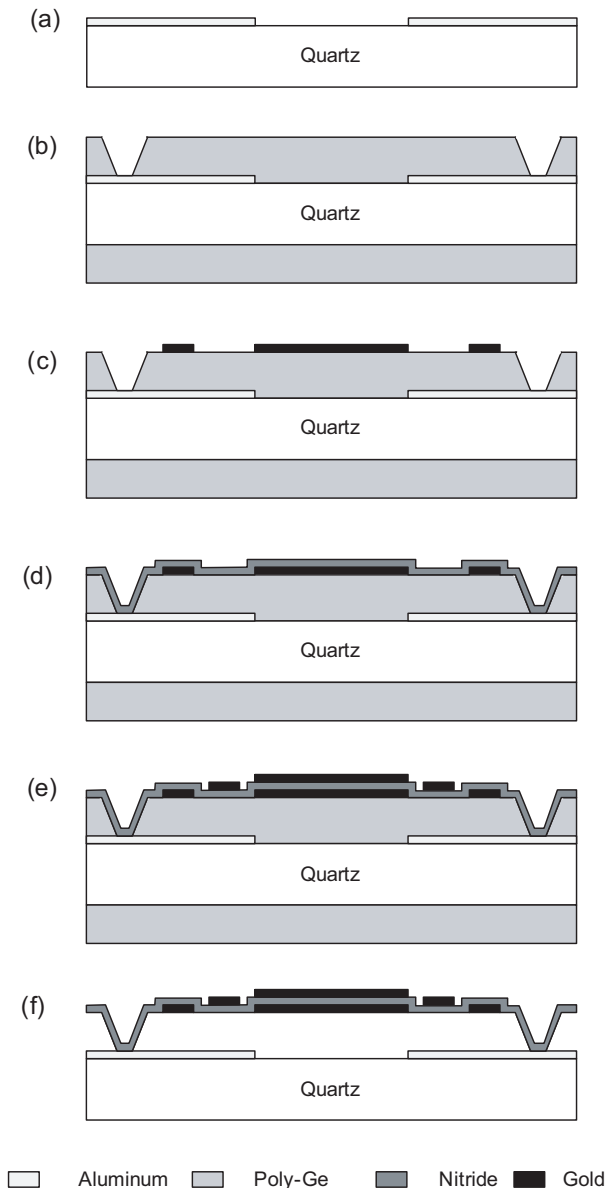


Fig. 7. Fabrication process: (a) aluminum evaporation and patterning for a fixed mirror (b) Poly-Ge LPCVD and patterning for anchors (c) Au-Cr layer evaporation and patterning by lift-off (d) PECVD silicon nitride deposition and patterning (e) Cr-Au layer evaporation and patterning by lift-off (f) sacrificial layer removal by XeF_2 etching

μm from the substrate. This initial position of the mirror comes from the stress gradient in the bi-material layers caused by the highly tensile residual stress of the metal thin film. Although our metal evaporation and silicon nitride deposition are quite uniform within a sensor region of $100\ \mu\text{m} \times 100\ \mu\text{m}$, there will be some minor deposition thickness and stress variation within the region. However, since the moving mirror is diagonally fixed by the two ends of bi-material sensing legs, it will be difficult to get a rotation motion. Through both the light micrograph and SEM, we couldn't observe any tilt of the moving mirror.

IV. EXPERIMENT

To check the operation and thermal response of the fabricated sensor, we performed a thermal response experiment using a commercial white light interferometry setup (VEECO Instruments

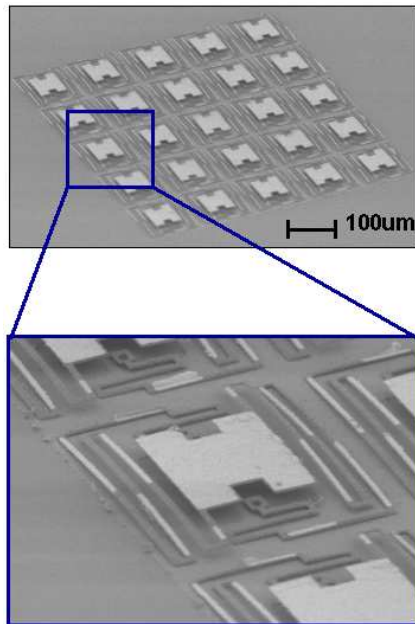


Fig. 8. Scanning electron micrograph of fabricated chip

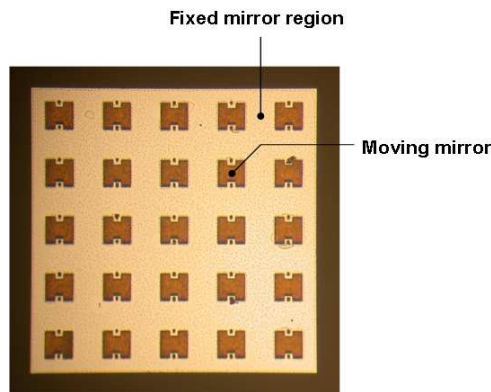


Fig. 9. Chip backside light micrograph through quartz substrate

Inc., Model WYKO NT3300) and a chip temperature control system, which consists of a thermistor, thermo-electric coolers, and temperature controller (Wavelength Electronics Inc., Model LFI-3751). In this experiment, the white light interferometer directly measures the movement of the moving mirror from the front side instead of measuring its motion through the quartz substrate. The heat of quartz substrate is easily transferred to the floated active sensor region by air conduction since the gap between the sensor region and the substrate is at most $13\ \mu\text{m}$. We waited for about 5 mins to achieve thermal equilibrium in each experiment. Fig. 10 shows the data of the moving mirror height measurements for various chip temperatures. As shown in this figure, it moves down as the chip temperature increases. However, there is small mirror height variation along the horizontal position. We think that it comes mainly from the measurement error due to the mirror surface roughness and the measurement imaging software. Although we observed a small thermally induced curvature change for the tested sensor, we think that its effect on optical interferometry is not critical. We assume that the light source from the measurement system is quite uniform. If it is non-uniform,

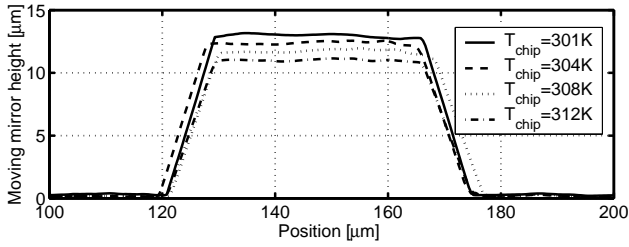


Fig. 10. Moving mirror height for chip temperature, T_{chip}

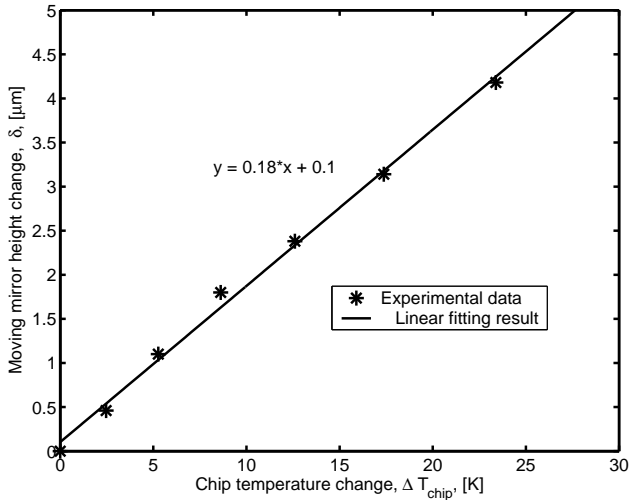


Fig. 11. Moving mirror height change δ (downward positive) vs. chip temperature change ΔT_{chip} : thermo-mechanical sensitivity $S_T = \delta/\Delta T_{\text{chip}} = 180\text{nm/K}$

there will be a temperature gradient on the mirror. This will affect the flatness or curvature of the mirror, which would have a detrimental effect on the measurement. Fig. 11 shows the sensor's mechanical sensitivity to chip temperature change, S_T . Each data point represents the change of the mirror average height at a given chip temperature change. For the tested temperature range, the performance results for several measurements were quite consistent. From the linear fitting result, the thermo-mechanical sensitivity, S_T , is 180 nm/K. The finite element simulation result, $S_T = 133\text{ nm/K}$, agrees within 26 % of this experimental result. We think the major difference can come from discrepancies in the material property values used in the finite element simulation. The experimental thermo-mechanical sensitivity value corresponds to the noise equivalent temperature resolution (or minimum detectable temperature change) of $\Delta T_n = h_n/S_T = 0.036\text{ nm}/180\text{ nm/K} = 200\text{ }\mu\text{K}$. This value can be increased by other noise sources like detector (or CCD) noise, measurement light source noise, etc. The consideration for all these noise sources is well documented in [1].

V. CONCLUSIONS

We proposed and fabricated a novel FOB beam to increase the deflection or sensitivity of micro-mechanical structures for temperature and surface stress change sensing. The FOB beam is configured such that a material layer coats half of the top surface of the beam at one section and half of the bottom surface at the opposite section. The FOB beam structure automatically satisfies the fixed-guided boundary condition due to

symmetry. Hence, the deflection of a single FOB beam can be approximated as the sum of two individual half beam deflections. Furthermore, the total deflection of multiply connected FOB beam structures can be approximated as the addition of each FOB beam deflection. Compared with a conventional bi-material beam design, having the same boundary conditions, the FOB beam has about 53 % higher mechanical sensitivity. Using the FOB beam design, we developed a micro-opto-mechanical sensor having a symmetric structure such that motion is converted into a linear displacement of a reflecting surface for interferometry. By multiple interconnections of FOB beams, we could amplify the deflection or sensitivity, and achieve the out-of-plane motion of a sensing structure. The designed sensor was fabricated by surface micromachining techniques using a transparent quartz substrate for optical measurement. To check the operation and thermal response of the fabricated sensor, we performed a thermal response experiment using a commercial white light interferometry setup and a chip temperature control system. Within a sensor area of $100\text{ }\mu\text{m} \times 100\text{ }\mu\text{m}$, the thermo-mechanical sensitivity $S_T = 180\text{ nm/K}$ was experimentally obtained.

ACKNOWLEDGMENT

The authors would like to thank Dr. John Kitching of National Institute of Standard and Technology and Dr. Thomas Thundat of Oak Ridge National Laboratory for many useful advices and support. We would also like to thank the Micro fabrication Laboratory, University of California, Berkeley, for providing micro fabrication facilities.

REFERENCES

- [1] Y. Zhao, M. Mao, R. Horowitz, A. Majumdar, J. Varesi, P. Norton, and J. Kitching, "Optomechanical uncooled infrared imaging system: Design, microfabrication, and performance," *Journal of Microelectromechanical Systems*, vol. 11, no. 2, pp. 136–146, 2002.
- [2] T. Thundat and A. Majumdar, *Microcantilevers for Physical, Chemical, and Biological Sensing: Sensors and Sensing in Biology and Engineering*. Springer-Verlag, 2003.
- [3] T. Thundat, E. Finot, Z. Hu, R. Ritchie, G. Wu, and A. Majumdar, "Chemical sensing in Fourier space," *Applied Physics Letter*, vol. 77, no. 24, pp. 4061–4063, 2000.
- [4] D. Baselt, B. Fruhberger, E. Klaassen, S. Cemalovic, C. B. Jr., S. Patel, T. Mlsna, D. McCorkle, and B. Warmack, "Design and performance of a microcantilever-based hydrogen sensor," *Sensors and Actuators B*, no. 88, pp. 120–131, 2003.
- [5] J. Fritz, M. Baller, H. Lang, H. Rothuizen, P. Vettiger, E. Meyer, H. Guntherodt, C. Gerber, and J. Gimzewski, "Translating biomolecular recognition into nanomechanics," *Science*, vol. 288, pp. 316–318, 2000.
- [6] G. Wu, R. Datar, K. Hansen, T. Thundat, R. Cote, and A. Majumdar, "Bioassay of prostate-specific antigen (PSA) using microcantilevers," *Nature Biotechnology*, vol. 19, pp. 856–860, 2001.
- [7] D. Sarid, *Scanning Force Microscopy*. Oxford University Press, 1994.
- [8] R. Raiteri, M. Grattarola, H. Butt, and P. Skladal, "Micromechanical cantilever-based biosensors," *Sensors and Actuators B*, vol. 79, pp. 115–126, 2001.
- [9] H.-F. Ji, K. Hansen, Z. Hu, and T. Thundat, "Detection of pH variation using modified microcantilever sensors," *Sensors and Actuators B*, no. 72, pp. 232–238, 2001.
- [10] G. Yaralioglu, A. Atalar, S. Manalis, and C. Quate, "Analysis and design of an interdigital cantilever as a displacement sensor," *Journal of Applied Physics*, vol. 83, no. 12, pp. 7405–7415, 1998.
- [11] W. Chu, M. Mehregany, and R. Mullen, "Analysis of tip deflection and force of a bimetallic cantilever microactuator," *Journal of Micromechanics and Microengineering*, vol. 3, pp. 4–7, 1993.
- [12] V. Pamula, A. Jog, and R. Fair, "Mechanical property measurement of thin-film gold using thermally actuated bimetallic cantilever beams," *Modeling and Simulation of Microsystems*, pp. 410–413, 2001.

- [13] T. Miyatani and M. Fujihira, "Calibration of surface stress measurements with atomic force microscopy," *Journal of Applied Physics*, vol. 81, no. 11, p. 70997115, 1997.
- [14] L. Kiesewetter, J. Zhang, D. Houdeau, and A. Steckenborn, "Determination of Young's moduli of micromechanical thin films using the resonance method," *Sensors and Actuators A*, vol. 35, pp. 153–159, 1992.
- [15] <http://www.memsnet.org>.
- [16] V. Ziebart, O. Paul, U. Munch, J. Schwizer, and H. Baltes, "Mechanical properties of thin films from the load deflection of long clamped plates," *Journal of Microelectromechanical Systems*, vol. 7, no. 3, pp. 320–328, 1998.



Si-Hyung Lim received the B.S. and M.S. degrees in Mechanical Design and Production Engineering at Seoul National University, Seoul, Korea in 1994 and 1996, respectively. He was a full-time instructor in Mechanical Engineering, Korea Air Force Academy, CheongWon, Korea (1998-2001). He is currently working towards the Ph.D. degree in Mechanical Engineering at University of California, Berkeley. His research interests include NEMS sensor and actuator development and its application.



Jongeun Choi received the BS degree in the Department of Mechanical Design and Production Engineering from the Yonsei University, Seoul, Korea, in 1998 and MS degree in the Department of Mechanical Engineering, at University of California, Berkeley. He is a PhD candidate in the same department from University of California, Berkeley. His research interests are control applications on MEMS sensor systems and sensor system design.



Roberto Horowitz received the B.S. degree with highest honors in Mechanical Engineering and the Ph.D. degree from the University of California, Berkeley, in 1978 and 1983, respectively. He is currently a Professor in the Department of Mechanical Engineering, University of California, Berkeley. He is teaching and conducting research in the areas of adaptive, learning, nonlinear and optimal control and mechatronics, with applications to disk file systems, robotics, MEMS, and intelligent vehicle and highway systems. He was the recipient of a 1984 IBM Young Faculty Development Award and a

1987 National Science Foundation Presidential Young Investigator Award.



Arunava Majumdar holds the Almy and Agnes Maynard Chair Professor in Mechanical Engineering, University of California, Berkeley, where he served as the vice chair from 1999-2002. He completed his PhD in Mechanical Engineering from UC Berkeley in 1989, and then served on the Mechanical Engineering faculties at Arizona State University (1989-92) and UC Santa Barbara (1992-96). He is a recipient of the NSF Young Investigator Award, the ASME Melville Medal, ASME Heat Transfer Division Best Paper Award, and 2001 ASME Gustus Larson Memorial Award. He is currently

serving as an editor for the International Journal of Heat and Mass Transfer, and co-editor-in-chief of *Microscale Thermophysical Engineering*. He also serves as Chair, Board of Advisors, ASME Nanotechnology Institute; Member, Council on Materials Science and Engineering, US Department of Energy; Member, Chancellor's Advisory Council on Nanoscience and Nanoengineering at UC Berkeley; and Member, Nanotechnology Technical Advisory Group to the President's Council of Advisors on Science and Technology (PCAST). He is a fellow member of both ASME and AAAS.